Recent Tests of QCD at SLD[*]

David Muller

Representing The SLD Collaboration[**]

Stanford Linear Accelerator Center
Stanford University, Stanford, CA 94309

Abstract

We present selected results on strong interaction physics from the SLD experiment at the SLAC Linear Collider. We report on several new studies of 3- and 4-jet hadronic Z^0 decays, in which jets are identified as quark, antiquark or gluon. The 3-jet $Z^0 \to b\bar{b}g$ rate is sensitive to the b-quark mass; prospects for measuring m_b are discussed. The gluon energy spectrum is measured over the full kinematic range, providing an improved test of QCD and limits on anomalous bbg couplings. The parity violation in $Z^0 \to b\bar{b}g$ decays is consistent with electroweak theory plus QCD. New tests of T- and CP-conservation at the bbg vertex are performed. A new measurement of the rate of gluon splitting into $b\bar{b}$ pairs yields $g_{b\bar{b}} = 0.0031 \pm 0.0007(stat.) \pm 0.0006(syst.)$ (Preliminary). We also present a number of new results on jet fragmentation into identified hadrons. The B hadron energy spectrum is measured over the full kinematic range using a new, inclusive technique, allowing stringent tests of predictions for its shape and a precise measurement of $\langle x_B \rangle = 0.714 \pm 0.005(stat.) \pm 0.007(syst.)$ (Preliminary). A detailed study of correlations in rapidity y between pairs of identified $\pi^\pm$, $K^\pm$ and p/$\bar{\text{p}}$ confirms that strangeness and baryon number are conserved locally, and shows local charge conservation between meson-baryon and strange-nonstrange pairs. Flavor-dependent long-range correlations are observed for all combinations of these hadron species, yielding new information on leading particle production. The first study of correlations using rapidities signed such that $y > 0$ corresponds to the quark direction provides additional new insights into fragmentation, including the first direct observation of baryon number ordering along the $q\bar{q}$ axis.

Presented at the 1999 International Euroconference on Quantum Chromodynamics,
7–13 July, 1999, Montpellier, France.

1.   Introduction

We present an overview of a number of recent measurements from the SLD experiment, using hadronic decays of Z^0 bosons produced in e^+e^- annihilations. First we present a number of precision tests of QCD in the perturbative regime using 3- and 4-jet final states. The goal here is sensitivity to radiative corrections to the reaction $e^+e^- \to Z^0/\gamma \to q\bar{q}(g)$ induced by known effects, such as the large mass of the b-quark, or by new physics. Such effects are expected at the few percent level, so the effects of higher order gluon radiation must be understood or suppressed at this level. Since we do not observe partons directly, rather the jets of particles into which they fragment, it is essential to understand the properties of these jets. Here we present two new, detailed studies of jet formation involving identified hadrons measured over a wide energy range.

A key to improving upon existing studies of multijet events has been the identification of the parton species that initiated a particular jet, or the identification of the primary q flavor in $e^+e^- \to q\bar{q}$. For example, the strong coupling α_s can be measured from R_3, the fraction of 3-jet $e^+e^- \to q\bar{q}g$ events, but the precision is limited by theoretical uncertainties to the level of $\sim 5\%$. However one can test the fundamental anzatz of flavor independence of α_s by comparing R_3 in events of different flavors so that many uncertainties cancel. The ratio $r^b = R_3^b/R_3^{uds}$ has been measured with sufficient precision that it is sensitive to the mass of the b-quark, m_b, introducing additional theoretical and experimental uncertainties. Here we review our latest measurements [1] of r^b, and discuss prospects for the precise measurement of m_b.

Experimental studies of the structure of 3-jet events have typically used energy and angle distributions of energy-ordered jets. Since the gluon is expected to be the lowest-energy jet in most events, this suffices to confirm the $q\bar{q}g$ origin of such events and to determine the gluon spin [2]. The identification of the three jets in such events would allow more complete and stringent tests of QCD. Here we present a study [3] of 3-jet final states in which two of the jets are tagged as b or $\bar{b}$ jets. The remaining jet is tagged as the gluon jet and its energy spectrum studied over the full kinematic range. Adding a tag of the charge of the b or $\bar{b}$ jet, and exploiting the high electron beam polarization of the SLC, we measure [4] two angular asymmetries sensitive to parity violation in the Z^0 decay, and also construct new tests of T- and CP-conservation at the bbg vertex.

The rate of secondary heavy flavor production via gluon splitting, $g \to c\bar{c}$, $g \to b\bar{b}$ is a sensitive test of QCD, as it is suppressed strongly by the mass of the heavy quark, but is still expected to be the dominant source of secondary heavy hadrons. Here we present a measurement of the $g \to b\bar{b}$ rate [5] that is complementary to other measurements in this rapidly emerging field.

The study of events containing $b/\bar{b}$ quarks is especially useful, both as important input into measurements such as electroweak parameters (R_b and A_b) in Z^0 decays and bottom production in hadron-hadron collisions, and also as a sensitive probe of any new physics that couples more strongly to heavier quarks.

The process of jet formation is not understood quantitatively, due to the difficulty of perturbative calculations in this soft regime. A number of phenomenological models

have been developed, and it is essential to understand the properties of jets empirically in order to test these models and encourage theoretical development. Since jets are used in many precision tests of electroweak and strong physics (e.g. those described below), and will constitute both the largest signal for and the background to any heavy particles discovered in the future, our understanding, even if only through models, must be as complete as possible.

The production of heavy hadrons from heavy primary quarks is relatively easy to calculate perturbatively due to the cutoff introduced by the large quark mass. A number of calculations and model predictions for the energy spectrum of bottom hadrons now exist and await precise testing. Experimental studies of the B-hadron spectrum have been limited by the efficiency for reconstructing the energies E_B of individual B hadrons with good resolution, especially for low-energy B hadrons. Here we present a study [6] of the E_B distribution using a novel kinematic technique and only charged tracks. The high efficiency and good resolution for all E_B, results in a measurement covering the full kinematic range.

Lighter identified particles are also an active field of study. The production of strange particles and baryons is of particular interest as they must be produced in strange-antistrange or baryon-antibaryon pairs, and the mechanism of their pair production can yield insights into the fragmentation process. Previous studies of rapidity correlations have shown that the conservation of such quantum numbers is predominantly local or short-range, i.e. the two particles are produced close together in the jet phase space. There is also evidence for long-range correlations from the leading particles in the two hemispheres of an event that contain the primary quark and antiquark.

Here we present detailed studies [7] of short- and long-range correlations between identified $\pi^\pm$, $K^\pm$ and p/$\bar{\text{p}}$ that improve substantially upon previous measurements. In addition, we use the SLC beam polarization to tag the quark hemisphere in each event and study for the first time rapidities signed such that positive (negative) rapidity corresponds to the (anti)quark hemisphere. Ordered differences in signed rapidity provide further unique insights into jet fragmentation, in particular being sensitive to local ordering of quantum numbers along the $q\bar{q}$ axis.

Unless otherwise noted, these measurements use the entire SLD hadronic sample of 550,000 events recorded from 1993 to 1998. Each exploits some of the unique feaures of the SLC/SLD program, such as the highly longitudinally polarized electron beam, small transverse beam size, and excellent vertex detection and particle identification. The magnitude of the beam polarization averaged 73%, providing high sensitivity to parity violating observables and a quark hemisphere tag of 73% purity. The collision region typically measured 0.8 μm vertically by 1.8 μm horizontally, which with the vertex detector gives a transverse impact parameter resolution of $\sigma_\delta = 8 \oplus 29/p \sin^{3/2}\theta$ μm, providing excellent heavy- and light-flavor tagging. We use a topological algorithm [8] that finds secondary vertices cleanly and efficiently, and also measures the flight direction independent of the momenta of the tracks in the vertex. Cutting on the vertex mass provides B (charmed) hadron samples of up to 98% (70%) purity. In addition we consider
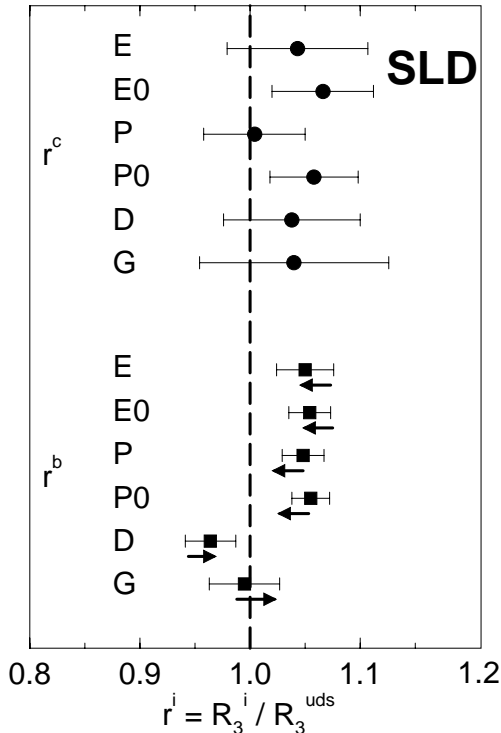
Figure 1: The measured 3-jet rate ratios r^c and r^b for six different jet finding algorithms. The predictions of the NLO QCD calculation of [10] are shown as the arrows whose tails (heads) represent an $m_b(m_Z)$ value of 3.5 (2.5) GeV/c^2.

the number of tracks in an event or jet, $n_{sig}^{(m)}$, that have a normalized transverse impact parameter wrt the interaction point (IP) of $\delta/\sigma_\delta > m$. Heavy hadron decays tend to give $n_{sig}^{(m)} > 0$, and the absence of such tracks provides an efficient light-flavor tag.

2. Flavor Independence and m_b

Well contained hadronic events [9] are selected and jets are counted in each using six collinear- and infrared-safe algorithms, with a set of optimized y_{cut} values. A combination [1] of the event $n_{sig}^{(2)}$ and the masses and momenta of the secondary vertices (if any) in each jet is used to tag each event as light(uds)-, c-, or b-flavor. The 3-jet rates R_3 in these three subsamples are unfolded for the effects of hadronization, detector efficiency and tagging efficiencies and biases, and the ratios $r^c = R_3^c/R_3^{uds}$ and $r^b = R_3^b/R_3^{uds}$ are shown in fig. 1.

All six r^c values are consistent with unity, however only one r^b value is within one standard deviation of unity. Furthermore the deviation from unity is different for different algorithms, and the six results show more scatter than would be expected given the high statistical correlation between them. This can be understood as an effect of the b-quark mass, m_b, which leads to a suppression of collinear gluon radiation, and also affects the

4

jetfinders directly, as they use the mass in different ways in their clustering metrics. There are several recent NLO calculations [10, 11] of the expected shift in r^b, which give consistent predictions. Those of [10] are shown as the arrows on fig. 1 for values of the running mass of $m_b(m_Z) = 3.0 \pm 0.5$ GeV/c^2; qualitative agreement with the data is evident.

We therefore used this prediction to extract ratios of the strong coupling:

$$\alpha_s^c/\alpha_s^{uds} = 1.036 \pm 0.043(stat.)^{+0.041}_{-0.045}(syst.)^{+0.020}_{-0.018}(theory)$$
$$\alpha_s^b/\alpha_s^{uds} = 1.004 \pm 0.018(stat.)^{+0.026}_{-0.031}(syst.)^{+0.018}_{-0.029}(theory),$$

using one-sixth of the data sample. The experimental uncertainty is expected to improve substantially when the entire sample is analyzed, and a dominant theoretical error on the latter ratio is from the uncertainty on $m_b(m_Z)$.

Recently, a number of groups [12, 13] have tried an alternative strategy of using these or similar data to measure $m_b(m_Z)$ assuming flavor independence of α_s. The experimental precision is already very good, however it is important to consider possible theoretical uncertainties. For example Brandenburg et al. have shown [12], using an updated calculation, that our six values of r^b are inconsistent if only experimental errors are considered. Postulating an additional 2% theoretical uncertainty due to uncalculated higher order terms, they extract

$$m_b(m_Z) = 2.56 \pm 0.27(stat.)^{+0.28}_{-0.38}(syst.)^{+0.49}_{-1.48}(theory) \ \ \text{GeV/c}^2,$$

where the latter error has large contributions from uncertainties in the hadronization correction as well as from the postulated theoretical uncertainty. If our theoretical knowledge is improved in these two areas, then this promises to provide a precise measurement of the b-quark mass.

3.   The Gluon Energy Spectrum

Hadronic events with exactly 3 jets (JADE algorithm, $y_{cut} = 0.02$) are selected. Jet energies E_i are calculated from the interjet angles [9], and the jets are energy ordered: $E_1 > E_2 > E_3$. We require $n_{sig}^{(3)} \geq 2$ in exactly two of the three jets, and the remaining jet is tagged as the gluon jet. This yields 8196 events with an estimated purity of correctly tagged gluon jets of 91%. In 3.0% (12.9%) of these events, jet 1(2), the (second) highest energy jet, is tagged as the gluon jet, giving coverage over the full kinematic range.

The distribution of the scaled gluon energy $x_g = 2E_g/\sqrt{s}$ is corrected [3] for non-$b\bar{b}g$ and mistag backgrounds, selection efficiency and resolution. The fully corrected spectrum, fig. 2, shows the expected falling behaviour with increasing x_g. It is cut off at low x_g by the finite y_{cut} value. Also shown are the predictions of first and second order QCD [10]; both describe the data in general, but not in detail. The prediction of the JETSET [14] parton shower simulation is also shown and reproduces the data. We thus confirm the
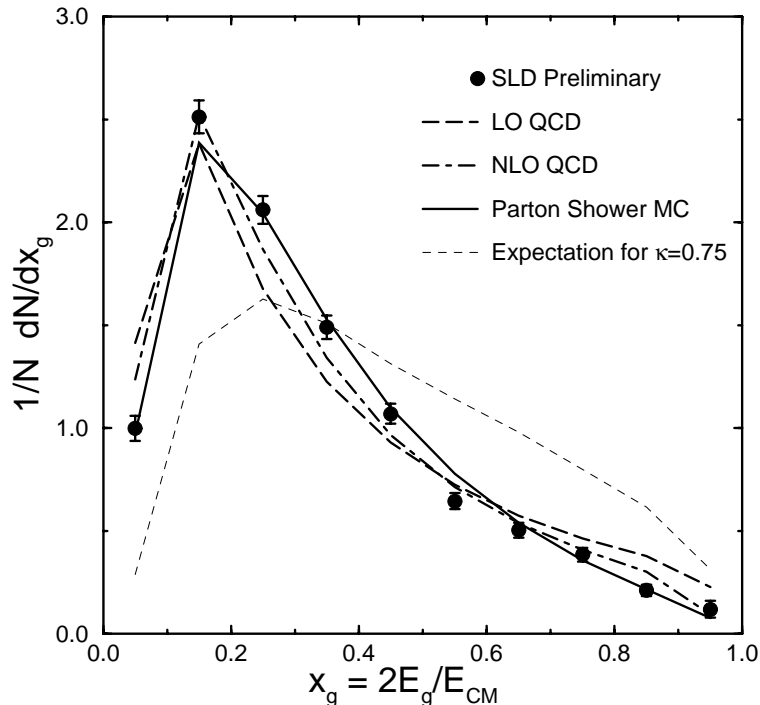
Figure 2: The fully corrected scaled gluon energy distribution (dots). The predictions of leading- and next-to-leading-order QCD and of a parton shower simulation are shown as the dashed, dot-dashed and solid lines, respectively. The thin dashed line shows the prediction for an anomalous chromomagnetic coupling at the bbg vertex with relative strength 0.75.

prediction of QCD, although higher order effects are clearly important in the intermediate gluon energy range, $0.2 < x_g < 0.4$.

The x_g spectrum is particularly sensitive to the presence of an anomalous chromomagnetic term in the strong interaction Lagrangian. A fit of the theoretical prediction [15] including an anomalous term parametrized by a relative coupling κ, yields a value of $\kappa = -0.01 \pm 0.05$ (Preliminary), consistent with zero, and corresponding to 95% C.L. limits on such contributions to the bbg coupling of $-0.11 < \kappa < 0.08$.

4.   Parity Violation in 3-Jet Z^0 Decays

We now consider two angles, the polar angle of the quark with respect to the electron beam direction θ_q, and the angle between the quark-gluon and quark-electron beam planes $\chi = \cos^{-1}(\hat{p}_q \times \hat{p}_g) \cdot (\hat{p}_q \times \hat{p}_e)$. The cosine x of each of these angles should be distributed as $1 + x^2 + 2A_P A_Z x$, where the Z^0 polarization $A_Z = (P_e - A_e)/(1 - P_e A_e)$ depends on that of the e^- beam P_e, and A_e and $A_P = A_0 A_q$ are predicted by QCD plus electroweak theory.

Three-jet events (Durham algorithm, $y_{cut} = 0.005$) are selected and energy ordered. The 14,658 events containing a secondary vertex with mass above 1.5 GeV/c^2 in any jet are kept, having an estimated $b\bar{b}g$ purity of 85%. We calculate the momentum-weighted
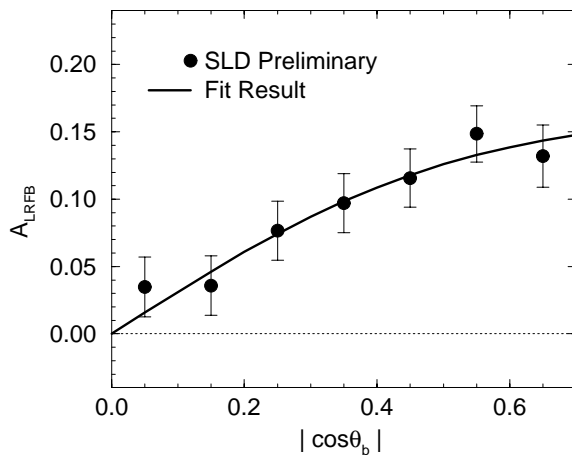
Figure 3: Left-right-forward-backward asymmetry of the b-quark polar angle in 3-jet Z^0 decays. The line is the result of a fit.
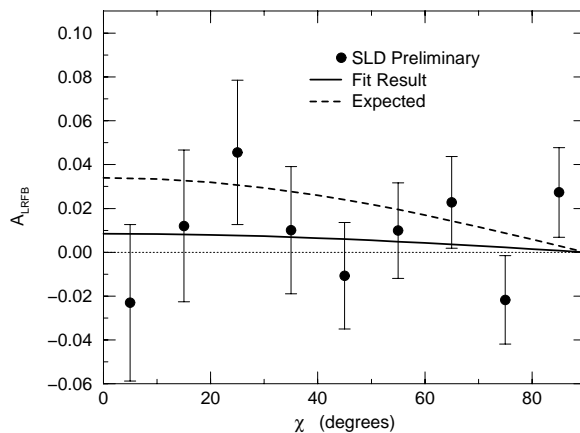

Figure 4: Left-right-forward-backward asymmetry of the angle χ in 3-jet Z^0 decays. The dashed and solid lines are the QCD prediction and the result of a fit, respectively.

charge of each jet j, $Q_j = \Sigma_i q_i |\vec{p}_i \cdot \hat{p}_j|^{0.5}$, using the charge q_i and momentum $\vec{p}_i$ of each track i in the jet. We assume that the highest-energy jet is not the gluon, and tag it as the b ($\bar{b}$) if $Q = Q_1 - Q_2 - Q_3$ is negative (positive). We define the b-quark polar angle by $\cos\theta_b = -\mathrm{sign}(Q)(\hat{p}_e \cdot \hat{p}_1)$.

The left-right-forward-backward asymmetry A^b_{LRFB} in $\cos\theta_b$ [4] is shown as a function of $|\cos\theta_b|$ in fig. 3. The clear asymmetry increases with increasing $|\cos\theta_b|$ in the expected way. A fit to the data yields an asymmetry parameter of $A_P = 0.91 \pm 0.05(stat.) \pm 0.06(syst.)$ (Preliminary), consistent with the QCD prediction of $A_P = 0.93 A_b = 0.87$.

We then tag one of the two lower energy jets as the gluon jet: if jet 2 has $n^{(3)}_{sig} = 0$ and jet 3 has $n^{(3)}_{sig} > 0$, then jet 2 is tagged as the gluon; otherwise jet 3 is tagged as the gluon. We construct the angle χ, and A^χ_{LRFB} is shown as a function of χ in fig. 4. Here we expect only a small deviation from zero as indicated by the dashed line on fig. 4. Our measurement is consistent with the prediction, as well as with zero. A fit yields $A_\chi = -0.014 \pm 0.035 \pm 0.002$ (Preliminary), to be compared with an expectation of -0.064.
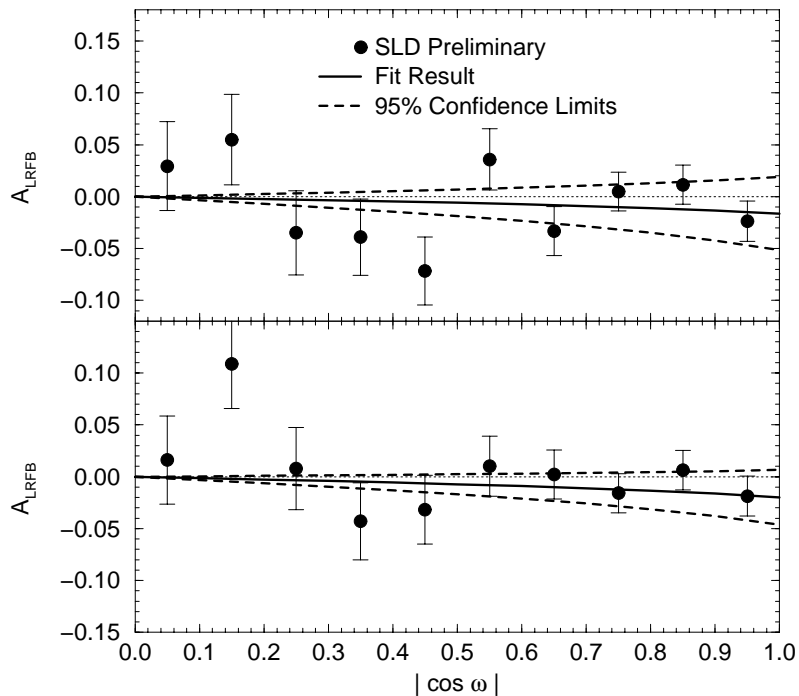
7

Figure 5: Left-right-forward-backward asymmetries of the energy- (top) and flavor-ordered (bottom) triple product. The solid (dashed) lines represent fits to the data (95% confidence limits).

5.   Symmetry Tests in $Z^0 \to b\bar{b}g$ Events

Using these fully tagged events, we can construct observables that are formally odd under time reversal and/or CP reversal. For example, the triple product $\cos\omega^+ = \vec{\sigma}_Z \cdot (\hat{p}_1 \times \hat{p}_2)$, formed from the directions of the Z^0 polarization $\vec{\sigma}_Z$ and the highest- and second highest-energy jets, is T_N-odd and CP-even. Since the true time reversed experiment is not performed, this quantity could have a nonzero A_{LRFB}, and we have previously set a limit [9] using events of all flavors. A calculation [16] including Standard Model final state interactions predicts that $A_{LRFB}^{\omega^+}$ is largest for $b\bar{b}g$ events, but is only $\sim 10^{-5}$. The fully flavor-ordered triple product $\cos\omega^- = \vec{\sigma}_Z \cdot (\hat{p}_q \times \hat{p}_{\bar{q}})$ is both T_N-odd and CP-odd.

Our measured $A_{LRFB}^{\omega^+}$ and $A_{LRFB}^{\omega^-}$ are shown in fig. 5. They are consistent with zero at all $|\cos\omega|$. Fits to the data yield 95% C.L. limits on any T_N-violating and CP-conserving or CP-violating asymmetries of $-0.038 < A_T^+ < 0.014$ or $-0.077 < A_T^- < 0.011$, respectively.

6.   Gluon Splitting into a $b\bar{b}$ Pair

Candidate events containing a gluon splitting into a $b\bar{b}$ pair, $Z^0 \to q\bar{q}g \to q\bar{q}b\bar{b}$, where the initial $q\bar{q}$ can be any flavor, are required to have 4 jets (Durham algorithm, $y_{cut} = 0.008$). A secondary vertex is required in each of the two jets with the smallest opening angle in the event, yielding 314 events. This sample is dominated by background, primarily from
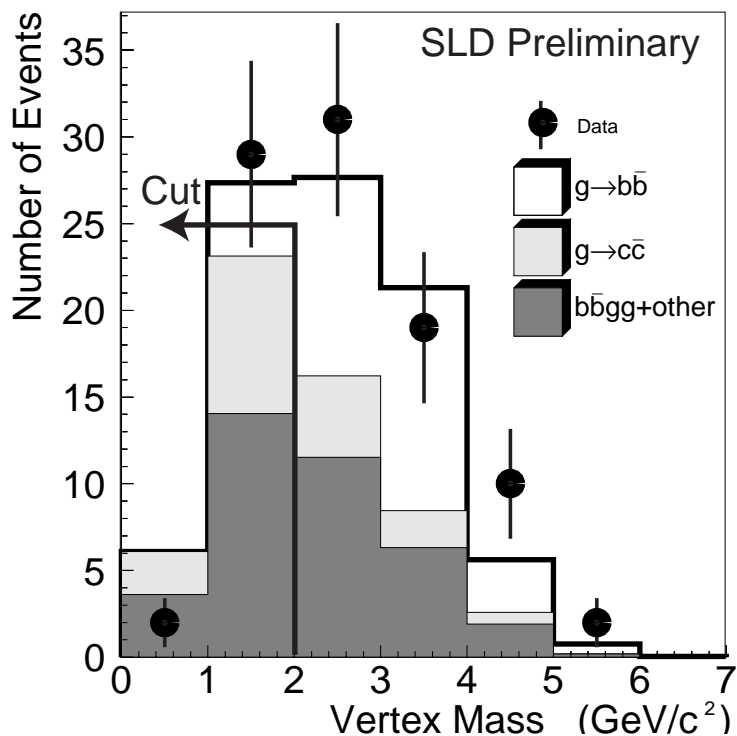
8

Figure 6: Distribution of the larger of the two vertex masses in candidate gluon splitting events after all other cuts (dots). The backgrounds expected from the simulation are indicated.

$Z^0 \to b\bar{b}g(g)$ events and events with a gluon splitting into a $c\bar{c}$ pair.

A large component of the former background is $Z^0 \to b\bar{b}g$ events in which the b or $\bar{b}$ jet is split into two jets by the jetfinder, and two distinct vertices from the *same* B-hadron decay are found. Since the small beam spot allows the vertex flight directions to be measured precisely, and the angle between the two flight directions from this background source tends to be small, it is suppressed by a cut on this angle.

Cuts are also made [5] on the sum of the energies of the two jets, the angle between the plane formed by the two selected jets and that formed by the other two jets in the event, and the larger of the vertex masses. The distribution of the latter quantity is shown in fig. 6 after all other cuts. A clear excess of events is visible over the expected background for masses above 2 GeV/c². A cut at this value keeps 62 events, with an estimated background of 27.6±1.2 events. Using this and the estimated efficiency for selecting $g \to b\bar{b}$ splittings of 3.9% yields a measured fraction of hadronic events containing such a splitting of

$$g_{b\bar{b}} = 0.0031 \pm 0.0007 \; (stat.) \pm 0.0006 \; (syst.)$$

(Preliminary). The systematic error is dominated by Monte Carlo statistics. The result is consistent with and complementary to previous measurements; in particular it is relatively insensitive to the modelling of the gluon splitting process, due to the excellent efficiency for finding vertices from low-energy B hadrons.

7. The B Hadron Energy Spectrum

Any secondary vertex in either thrust hemisphere of an event that has $m > 2$ GeV/c^2 is considered as a candidate B-hadron vertex. Its flight direction is taken to be along the line joining the IP and the vertex position. The four-vector sum of the tracks in the vertex (assigned the charged pion mass) is calculated, and the momentum component P_t transverse to the flight direction is equated with the transverse component of the "missing" momentum. At this point two quantities are still needed in order to determine the energy E_B of the B hadron, the missing mass M_0 and momentum along the flight direction. Assuming a B hadron mass of M_B eliminates one of these unknowns, and also allows an upper limit to be calculated on M_0:

$$M_{0max}^2 = M_B^2 - 2M_B\sqrt{M_{chg}^2 + P_t^2} + M_{chg}^2,$$

where M_{chg} is the mass of the set of tracks in the vertex. Using $M_B = 5.28$ GeV/c^2, equating M_0^2 with M_{0max}^2 and solving for E_B provides a good estimate of the true E_B for the mixture of B species produced in Z^0 decays. As expected, the simulated energy resolution is best for vertices with small M_{0max}^2, approaching 6% as $M_{0max}^2 \to 0$. It does not degrade rapidly with increasing M_{0max}^2 due to the strong tendency for the true M_0 to cluster near the maximum value.

A cut is placed on M_{0max}^2 that depends on the measured E_B in such a way that the simulated efficiency for selecting B vertices is roughly independent of energy; it is 4% on average and is above 3% for $E_B > 8$ GeV. A sample of 1938 vertices is selected from one-third of the hadronic event sample, with an estimated B-hadron purity of 99.5%. The simulated energy resolution is 10% on average, roughly independent of E_B. The raw distribution of the scaled energy $x_B = E_B/E_{beam}$ is shown in fig. 7, and covers the entire kinematic range from the B-hadron mass ($x_B \approx 0.12$) to the beam energy.

Also shown in fig. 7 is the prediction of our simulation, generated using the JETSET program with the Peterson fragmentation option and $\epsilon_b = 0.006$. The predicted peak position is consistent with that of the data, but the width is significantly larger than that of the data.

The correction of these data to obtain the true x_B distribution depends on the form assumed for the true distribution, due to the rapid variation of the distribution on the scale of the bin size. We therefore test several hypothesized shapes by weighting our simulated events to reproduce a given function at the generator level, and comparing the corresponding detector level prediction with the data in fig. 7 using a binned χ^2.

We first consider a number of heavy-hadron fragmentation models within the context of the JETSET simulation, by generating samples of 0.5 million $Z^0 \to b\bar{b}$ events for each of several values of the free parameters of each model. Minimizing χ^2 with respect to the parameter ϵ_b of the Peterson function results in a fitted value of $\epsilon_b = 0.006$, equal to our nominal value; however the χ^2 of 62 for 16 degrees of freedom indicates that this model is inconsistent with the data. We also exclude [6] the models of Braaten et. al, and Collins and Spiller, whereas those of the Lund group, Bowler, and Kartvelishvili are
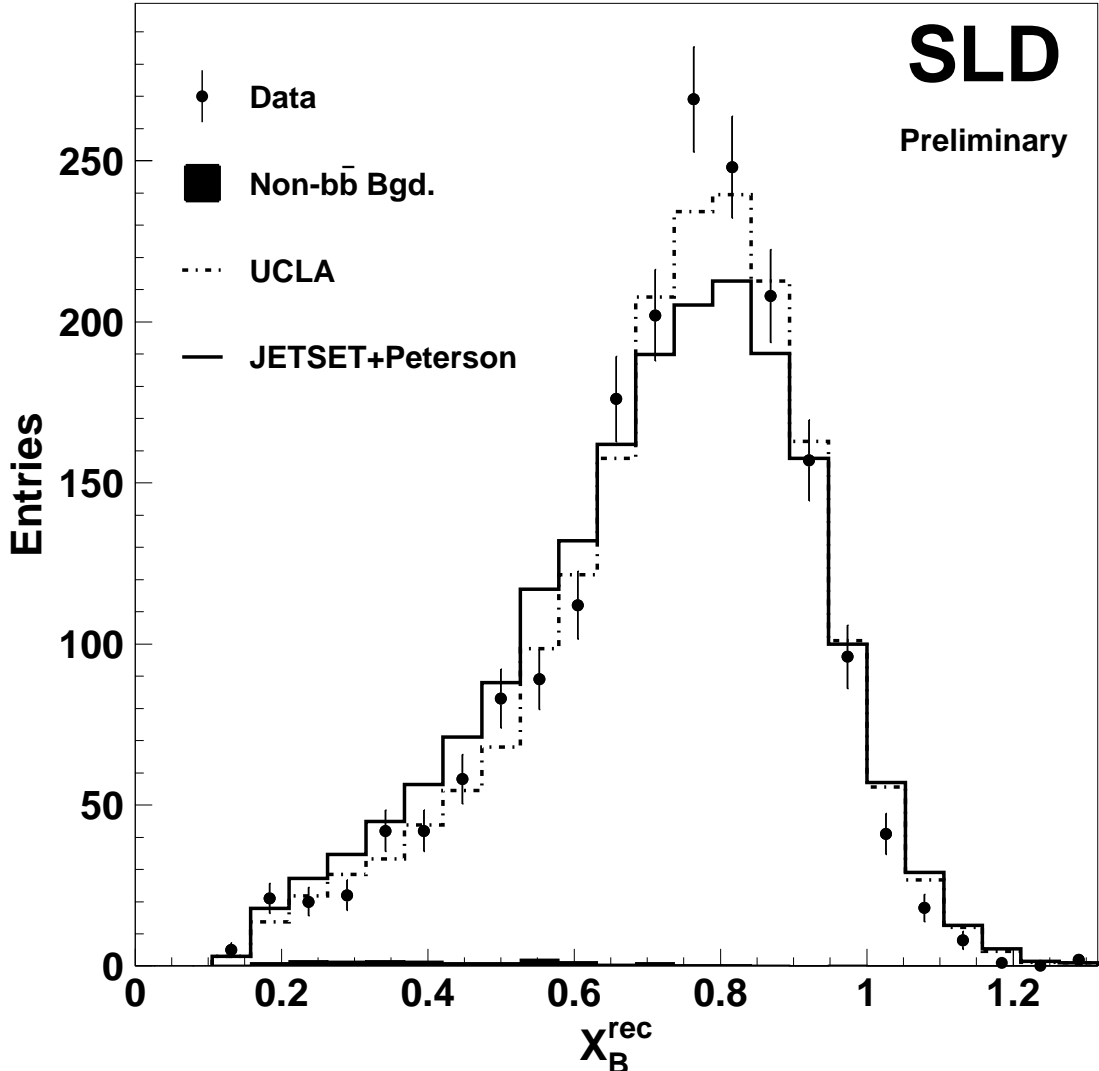
Figure 7: Uncorrected distribution of reconstructed B-hadron energies (dots). The solid (dot-dashed) histogram is the prediction of the JETSET+Peterson (UCLA) simulation.

able to describe the data. In addition we test the UCLA and HERWIG fragmentation models, in which there are no explicit free parameters governing B hadron production. The prediction of the UCLA model (see fig. 7) is consistent with the data, but that of the HERWIG model is not.

We also test several ad hoc functional forms $f(x_B, \vec{\lambda})$ of the observable x_B itself, by minimizing χ^2 with respect to the parameter(s) $\vec{\lambda}$. Most of our test functions [6] are not able to describe the data for any values of their parameters. Four functions, the Peterson function, two generalizations thereof, and a sixth order polynomial, are found to describe the data.

We subtract the estimated background and unfold the data to obtain the true distribution $D_i^{corr} = \Sigma_k M_{ik} D_k^{meas}/\epsilon_i$, where the efficiency $\vec{\epsilon}$ and the unfolding matrix $\mathbf{M}$ are
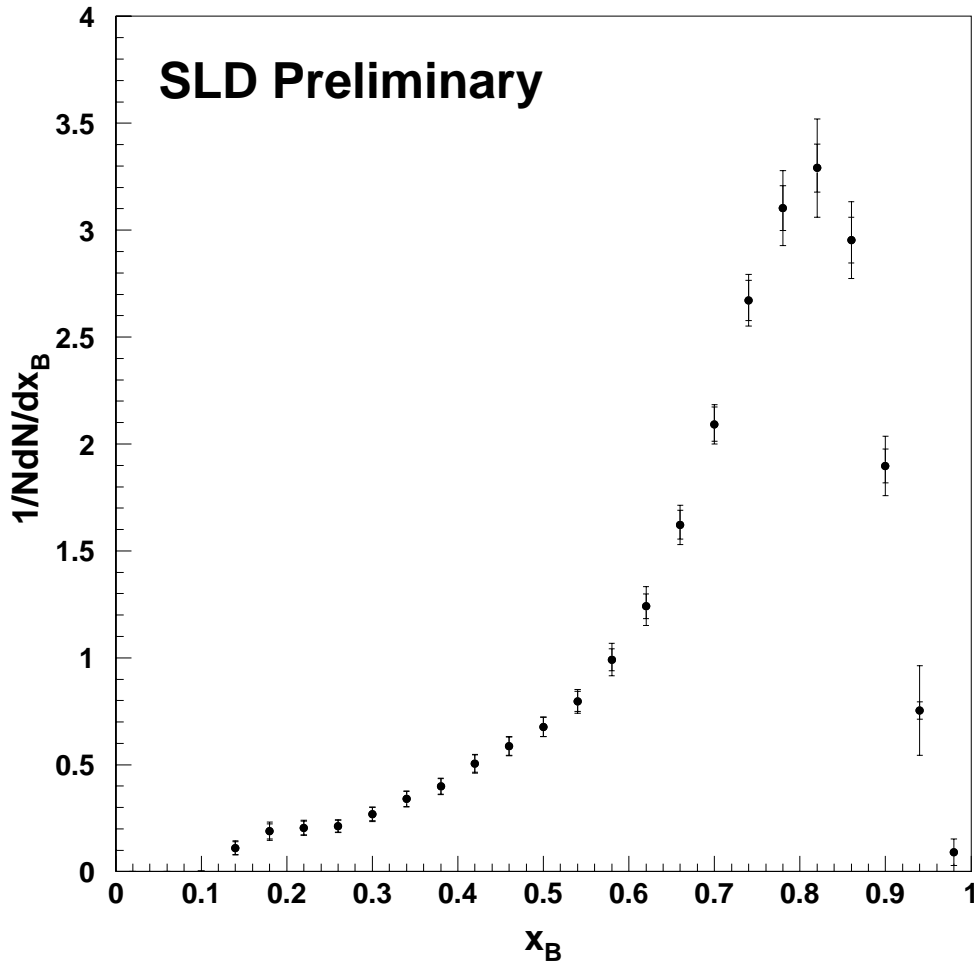
11

Figure 8: Corrected distribution of B-hadron energies averaged over the eight acceptable shapes. The outer error bars include the rms deviation among these shapes and provide an envelope for the true shape of the distribution.

calculated from the simulation using in turn each of the four fragmentation models and four functional forms that are consistent with the data. The model dependence of the procedure is thus made explicit, and is visible in fig. 8, where in each bin i we show the average of the eight D_i^{corr}, and the error bar includes their rms deviation, which is substantial at high x_B. The corrected distribution is, by construction, smoother than the measured distribution, and the error bars provide a 1σ envelope within which any acceptable prediction must fall.

From these eight forms we extract a measurement of the mean value of the scaled energy,

$$\langle x_B \rangle = 0.714 \pm 0.005(stat.) \pm 0.007(syst.) \pm 0.002(rms)$$

(Preliminary). This is the most precise of the world's measurements that take the shape dependence into account, and this uncertainty is small since we are able to exclude a wide range of shapes.
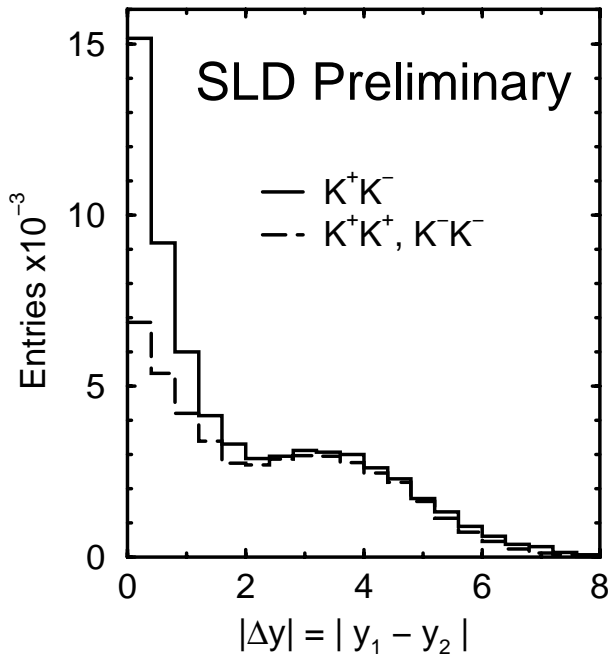
Figure 9: Distributions of the absolute rapidity difference $|\Delta y|$ for opposite-charge (histogram) and same-charge (dashed histrogram) pairs of identified charged kaons in hadronic Z^0 decays.

8.   Rapidity Correlations

For this study [7] we use the entire sample of hadronic events, as well as subsamples tagged as primary light-(uds), c-, and b-flavor, having purities of 88%, 39%, and 93%, respectively. Charged tracks identified as $\pi^\pm$, $K^\pm$ or p/$\bar{\text{p}}$ in the CRID are considered, and their rapidities $y = 0.5\ln((E + p_\parallel)/(E - p_\parallel))$ are calculated using their measured energies and components of momentum along the event thrust axis $p_\parallel$. For each pair of identified tracks in an event the absolute value of the difference between their rapidities $|\Delta y| = |y_1 - y_2|$ is considered. Figure 9 shows the distributions of $|\Delta y|$ for identified K^+K^- pairs and for K^+K^+/K^-K^- pairs. The latter are assumed to be uncorrelated, and the excess of the former at low values of $|\Delta y|$ is interpreted as a short-range correlation, indicating that strangeness conservation is local in the jet fragmentation process. This is also the case for baryon number and electric charge, as is well known and visible in fig. 10, which shows the difference between the opposite-charge and same-charge distributions for all six pair combinations.

Also visible in fig. 10 are short-range correlations for all three unlike pair combinations. Excellent particle identification is required to observe these over the background from $\pi\pi$ pairs in which one of the pions is misidentified. This is the first direct observation of a fundamental feature of the jet fragmentation process, that electric charge can be conserved locally between a meson and a baryon, or between a strange particle and a nonstrange particle, and suggests charge ordering along the entire fragmentation chain.

The high statistics and wide momentum coverage allow a number of detailed measure-
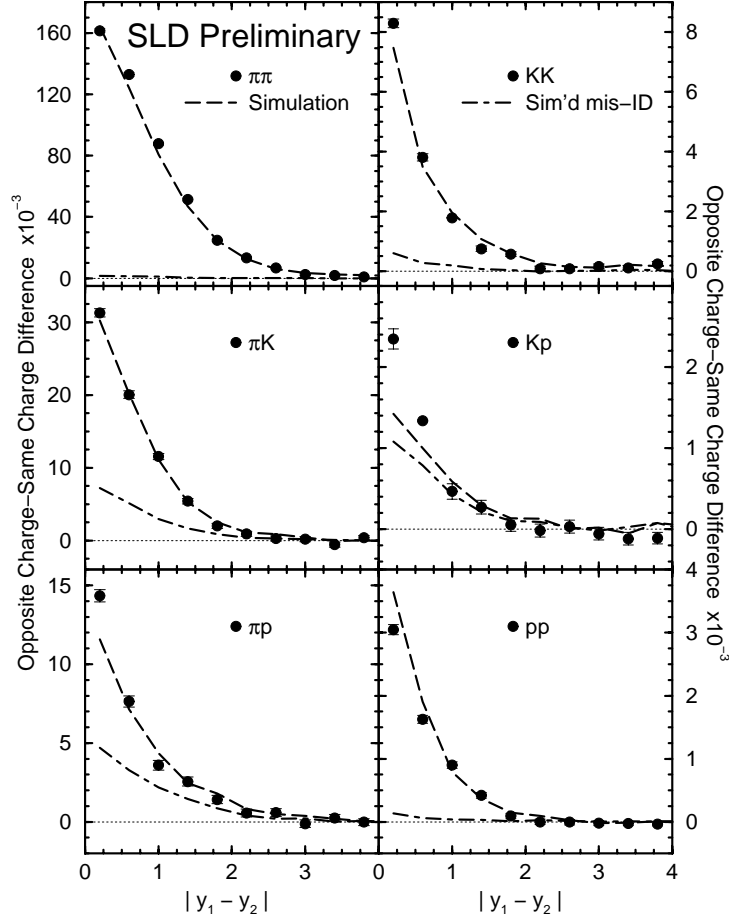
Figure 10: Differences between the $|\Delta y|$ distributions for opposite- and same-charge pairs of identified $\pi^{\pm}$, $K^{\pm}$, p/$\bar{\text{p}}$ in hadronic Z^0 decays (dots). The dashed (dot-dashed) lines indicate the simulated differences (contributions from pairs with a misidentified track).

ments. The predictions of the JETSET model (see fig. 10) describe the amplitude and range of the observed correlations except for Kp pairs. This is true in six bins of momentum [7], and we conclude that, within the context of the JETSET model, the correlations are scale invariant.

To study long-range correlations, which are expected from leading particle production, it is necessary to consider high momentum tracks. The differences between the opposite- and same-charge $|\Delta y|$ distributions for pairs of tracks in which both have $p > 9$ GeV/c are shown for each of the three flavor-tagged samples in fig. 11. A very large K^+K^- correlation is observed in light-flavor events, as expected from $s\bar{s}$ events in which the s ($\bar{s}$) jet produces a leading K^- (K^+). For all other combinations, any correlation will be diluted by the short-range correlation – e.g. a leading baryon will be accompanied by a subleading antibaryon with similar y. However significant correlations are observed for all pair combinations in light flavor events, providing new information on leading particle production. The JETSET model predictions are consistent with these data [7], except
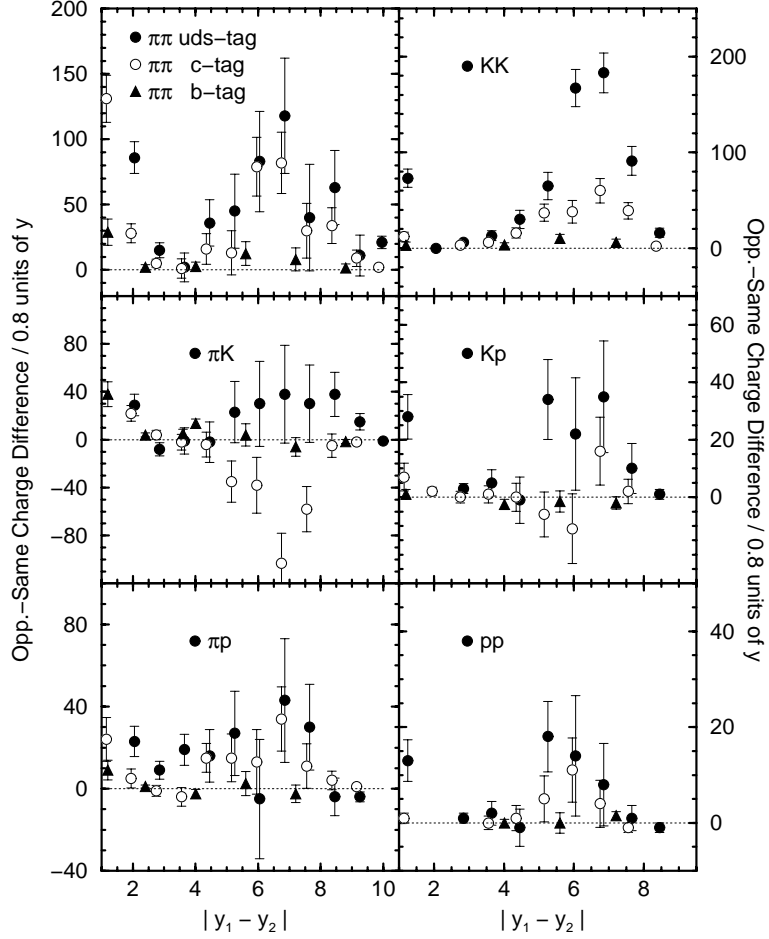
Figure 11: Differences between the $|\Delta y|$ distributions for opposite-charge and same-charge pairs in which both tracks have $p > 9$ GeV/c, for the light-(dots), c-(open circles), and b-tagged (triangles) samples.

that no πK correlation is predicted. Flavor tagging is essential for these measurements; decays of leading charmed hadrons contribute to several correlations, in particular they give an anticorrelation for πK pairs that would mask the signal from light flavors.

We now give the rapidity a meaningful sign by using the beam polarization to tag the quark hemisphere in each event, with a purity of 73%. The thrust axis is signed to point into this hemisphere, thus signing the rapidity such that $y > 0$ ($y < 0$) in the (anti)quark hemisphere. For pairs of hadrons one can define an ordered rapidity difference; for hadron-antihadron pairs we define $\Delta y^{+-} = y_+ - y_-$ as the rapidity of the positively charged track minus that of the negative track.

A distribution of Δy^{+-} can be studied independent of the same-charge pairs by considering asymmetries between the positive and negative sides of the distribution. In fig. 12 we show the distributions of Δy^{+-}, along with the differences between the two sides, for $\pi^+\pi^-$, K^+K^- and p$\bar{\text{p}}$ pairs, which show a number of nonzero asymmetries. At long-range ($|\Delta y^{+-}| > 3$), such deviations are expected from leading particle production. A large
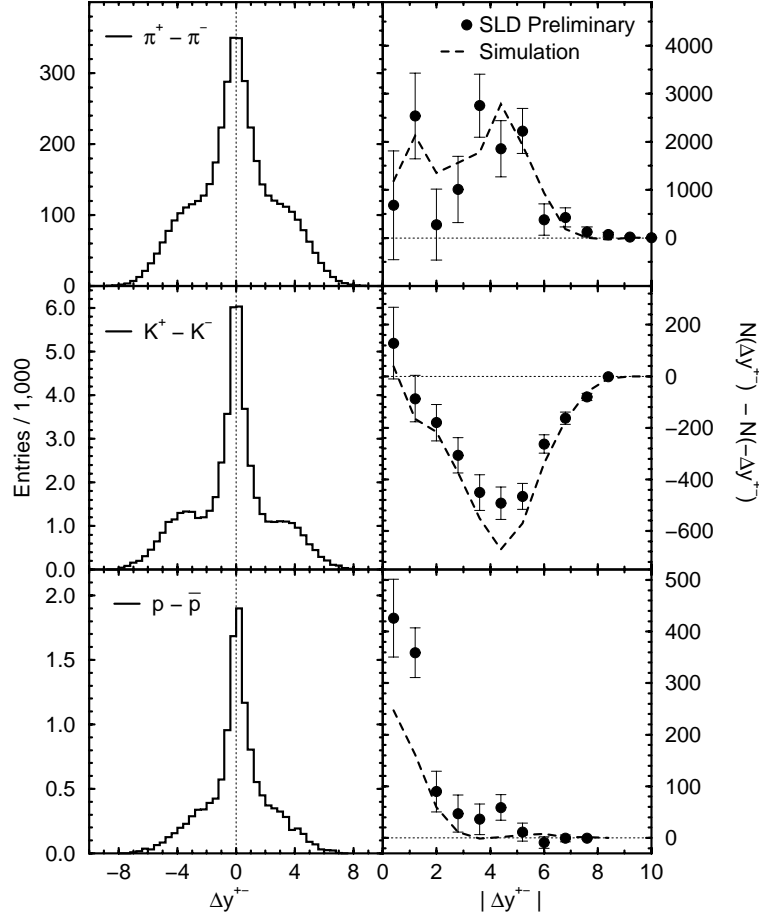
15

Figure 12: Distributions (left) of the ordered signed rapidity difference Δy^{+-}, and differences (right) between the positive and negative sides of each distribution. The dashed lines indicate the predictions of the JETSET simulation.

negative difference is observed for K^+K^- pairs, as expected; a corresponding small positive difference is visible for $p\bar{p}$ pairs, but a small negative difference for $\pi^+\pi^-$ pairs is not. Flavor tagging again proves beneficial: the positive differences at all $|\Delta y^{+-}|$ are present only in the c-tagged sample, and are explained by the leading charmed hadrons; a small negative difference is observed in the light-flavor sample [7].

The large positive difference observed for $p\bar{p}$ pairs at low $|\Delta y^{+-}|$ is the first direct observation of another fundamental feature of jet fragmentation, namely the ordering of baryon number along the quark-antiquark axis. That is, the proton in a correlated proton-antiproton pair 'knows' and prefers the quark direction over the antiquark direction. This excess is observed at all proton momenta so cannot be attributed simply to leading baryons. We have searched for similar signals for strangeness and charge ordering in the K^+K^- and $\pi^+\pi^-$ samples, respectively, by isolating the light flavors and considering a variety of momentum bins. However no significant effects are observed, possibly due to background from leading kaons and/or dilution due to resonance decays.

9. Conclusions

We use the excellent SLD vertexing and particle identificaton, and the high SLC e^- beam polarization to make several new tests of QCD in the two areas of event structure and jet fragmentation. We find the $Z^0 \to b\bar{b}g$ rate to be sensitive to the b-quark mass, providing a promising new way to measure m_b. Using 3-jet final states in which jets are tagged as b, $\bar{b}$ or gluon jets: we measure the gluon energy spectrum over its full range, confirming the prediction of QCD and setting limits on anomalous chromomagnetic couplings; we find the parity violation in $Z^0 \to b\bar{b}g$ decays to be consistent with electroweak theory plus QCD; and we perform new tests of T- and CP-conservation in strong interactions. Using 4-jet final states in which the two most collinear jets are tagged as $b/\bar{b}$, we measure the rate of gluon splitting into a $b\bar{b}$ pair in hadronic Z^0 decays, $g_{b\bar{b}} = 0.0031 \pm 0.0007(stat.) \pm 0.0006(syst.)$ (Preliminary).

A new, inclusive technique for measuring the energies of individual B hadrons uses information only from the charged tracks attached to a secondary vertex to give good efficiency and resolution at all energies. The full B-hadron energy distribution is measured precisely, allowing us to test a number of model predictions and ad hoc functional forms. We exclude a wide range of forms, constrain the shape tightly, and obtain a precise measurement of the average scaled energy, $\langle x_B \rangle = 0.714 \pm 0.005(stat.) \pm 0.007(syst.) \pm 0.002$ (*shape*) (Preliminary).

Considering pairs of identified $\pi^\pm$, $K^\pm$ and p/$\bar{\text{p}}$, we confirm that the conservation of quantum numbers is local in the jet fragmentation process, and observe local charge conservation between mesons and baryons and between strange and nonstrange particles. Long range correlations are also observed between all these pair combinations, providing new information on leading particle production. The first study of ordered correlations in signed rapidity provides additional new information on fragmentation, including the first direct observation of baryon number ordering along the quark-antiquark axis.

References

[1] K. Abe, et al., Phys. Rev. **D59** (1999) 12002.

[2] K. Abe, et al., Phys. Rev. **D55** (1997) 2533.

[3] SLD Collab., K. Abe et al., SLAC-Pub-8155, EPS-HEP99-1_182, hep-ex/9908031.

[4] SLD Collab., K. Abe et al., SLAC-Pub-8156, EPS-HEP99-1_183, hep-ex/9908028.

[5] SLD Collab., K. Abe et al., SLAC-Pub-8157, EPS-HEP99-1_184, hep-ex/9908032.

[6] SLD Collab., K. Abe et al., SLAC-Pub-8153, EPS-HEP99-1_185, hep-ex/9908035.

[7] SLD Collab., K. Abe et al., SLAC-Pub-8160, EPS-HEP99-1_187, hep-ex/9908027.

[8] D.J. Jackson, Nucl. Inst. Meth. **A388** (1997) 247.

[9] K. Abe, et al., Phys. Rev. Lett. **75** (1996) 4173.

[10] W. Bernreuther, A. Brandenburg, P. Uwer, Phys. Rev. Lett. **79** (1997) 189;
A. Brandenburg, P. Uwer, Nucl. Phys. **B515** (1998) 279.

[11] G. Rodrigo, A. Santamaria, M. Bilenky, Phys. Rev. Lett. **79** (1997) 193;
P. Nason, C. Oleari, Phys. Lett. **B407** (1997) 57; Nucl. Phys. **B521** (1998) 237.

[12] A. Brandenburg, P.N. Burrows, D. Muller, N. Oishi and P. Uwer, to appear in Physics Letters **B**.

[13] DELPHI Collab., P. Abreu, et al., Phys. Lett. **B418** (1998) 430;
ALEPH Collab., EPS-HEP99-1_384.

[14] T. Sjöstrand, Cmp. Ph. Comm. **82** (1994) 74.

[15] T. Rizzo, Phys. Rev. **D50** (1994) 4478.

[16] A. Brandenburg, L. Dixon and Y. Shadmi, Phys. Rev. **D53** (1996) 1264.

**List of Authors

Kenji Abe,[21] Koya Abe,[33] T. Abe,[29] I.Adam,[29] T. Akagi,[29] N. J. Allen,[5] W.W. Ash,[29] D. Aston,[29] K.G. Baird,[17] C. Baltay,[40] H.R. Band,[39] M.B. Barakat,[16] O. Bardon,[19] T.L. Barklow,[29] G. L. Bashindzhagyan,[20] J.M. Bauer,[18] G. Bellodi,[23] R. Ben-David,[40] A.C. Benvenuti,[3] G.M. Bilei,[25] D. Bisello,[24] G. Blaylock,[17] J.R. Bogart,[29] G.R. Bower,[29] J. E. Brau,[22] M. Breidenbach,[29] W.M. Bugg,[32] D. Burke,[29] T.H. Burnett,[38] P.N. Burrows,[23] A. Calcaterra,[12] D. Calloway,[29] B. Camanzi,[11] M. Carpinelli,[26] R. Cassell,[29] R. Castaldi,[26] A. Castro,[24] M. Cavalli-Sforza,[35] A. Chou,[29] E. Church,[38] H.O. Cohn,[32] J.A. Coller,[6] M.R. Convery,[29] V. Cook,[38] R. Cotton,[5] R.F. Cowan,[19] D.G. Coyne,[35] G. Crawford,[29] C.J.S. Damerell,[27] M. N. Danielson,[8] M. Daoudi,[29] N. de Groot,[4] R. Dell'Orso,[25] P.J. Dervan,[5] R. de Sangro,[12] M. Dima,[10] A. D'Oliveira,[7] D.N. Dong,[19] M. Doser,[29] R. Dubois,[29] B.I. Eisenstein,[13] V. Eschenburg,[18] E. Etzion,[39] S. Fahey,[8] D. Falciai,[12] C. Fan,[8] J.P. Fernandez,[35] M.J. Fero,[19] K.Flood,[17] R. Frey,[22] J. Gifford,[36] T. Gillman,[27] G. Gladding,[13] S. Gonzalez,[19] E. R. Goodman,[8] E.L. Hart,[32] J.L. Harton,[10] A. Hasan,[5] K. Hasuko,[33] S. J. Hedges,[6] S.S. Hertzbach,[17] M.D. Hildreth,[29] J. Huber,[22] M.E. Huffer,[29] E.W. Hughes,[29] X.Huynh,[29] H. Hwang,[22] M. Iwasaki,[22] D. J. Jackson,[27] P. Jacques,[28] J.A. Jaros,[29] Z.Y. Jiang,[29] A.S. Johnson,[29] J.R. Johnson,[39] R.A. Johnson,[7] T. Junk,[29] R. Kajikawa,[21] M. Kalelkar,[28] Y. Kamyshkov,[32] H.J. Kang,[28] I. Karliner,[13] H. Kawahara,[29] Y. D. Kim,[30] M.E. King,[29] R. King,[29] R.R. Kofler,[17] N.M. Krishna,[8] R.S. Kroeger,[18] M. Langston,[22] A. Lath,[19] D.W.G. Leith,[29] V. Lia,[19] C.Lin,[17]

M.X. Liu,[40] X. Liu,[35] M. Loreti,[24] A. Lu,[34] H.L. Lynch,[29] J. Ma,[38]
G. Mancinelli,[28] S. Manly,[40] G. Mantovani,[25] T.W. Markiewicz,[29]
T. Maruyama,[29] H. Masuda,[29] E. Mazzucato,[11] A.K. McKemey,[5] B.T. Meadows,[7]
G. Menegatti,[11] R. Messner,[29] P.M. Mockett,[38] K.C. Moffeit,[29] T.B. Moore,[40]
M.Morii,[29] D. Muller,[29] V.Murzin,[20] T. Nagamine,[33] S. Narita,[33] U. Nauenberg,[8]
H. Neal,[29] M. Nussbaum,[7] N.Oishi,[21] D. Onoprienko,[32] L.S. Osborne,[19]
R.S. Panvini,[37] C. H. Park,[31] T.J. Pavel,[29] I. Peruzzi,[12] M. Piccolo,[12]
L. Piemontese,[11] K.T. Pitts,[22] R.J. Plano,[28] R. Prepost,[39] C.Y. Prescott,[29]
G.D. Punkar,[29] J. Quigley,[19] B.N. Ratcliff,[29] T.W. Reeves,[37] J. Reidy,[18]
P.L. Reinertsen,[35] P.E. Rensing,[29] L.S. Rochester,[29] P.C. Rowson,[9] J.J. Russell,[29]
O.H. Saxton,[29] T. Schalk,[35] R.H. Schindler,[29] B.A. Schumm,[35] J. Schwiening,[29]
S. Sen,[40] V.V. Serbo,[29] M.H. Shaevitz,[9] J.T. Shank,[6] G. Shapiro,[15]
D.J. Sherden,[29] K. D. Shmakov,[32] C. Simopoulos,[29] N.B. Sinev,[22] S.R. Smith,[29]
M. B. Smy,[10] J.A. Snyder,[40] H. Staengle,[10] A. Stahl,[29] P. Stamer,[28] H. Steiner,[15]
R. Steiner,[1] M.G. Strauss,[17] D. Su,[29] F. Suekane,[33] A. Sugiyama,[21] S. Suzuki,[21]
M. Swartz,[14] A. Szumilo,[38] T. Takahashi,[29] F.E. Taylor,[19] J. Thom,[29]
E. Torrence,[19] N. K. Toumbas,[29] T. Usher,[29] C. Vannini,[26] J. Va'vra,[29]
E. Vella,[29] J.P. Venuti,[37] R. Verdier,[19] P.G. Verdini,[26] D. L. Wagner,[8]
S.R. Wagner,[29] A.P. Waite,[29] S. Walston,[22] J.Wang,[29] S.J. Watts,[5]
A.W. Weidemann,[32] E. R. Weiss,[38] J.S. Whitaker,[6] S.L. White,[32] F.J. Wickens,[27]
B. Williams,[8] D.C. Williams,[19] S.H. Williams,[29] S. Willocq,[17] R.J. Wilson,[10]
W.J. Wisniewski,[29] J. L. Wittlin,[17] M. Woods,[29] G.B. Word,[37] T.R. Wright,[39]
J. Wyss,[24] R.K. Yamamoto,[19] J.M. Yamartino,[19] X. Yang,[22] J. Yashima,[33]
S.J. Yellin,[34] C.C. Young,[29] H. Yuta,[2] G. Zapalac,[39] R.W. Zdarko,[29] J. Zhou.[22]

[1]*Adelphi University, Garden City, New York 11530,*
[2]*Aomori University, Aomori , 030 Japan,*
[3]*INFN Sezione di Bologna, I-40126, Bologna Italy,*
[4]*University of Bristol, Bristol, U.K.,*
[5]*Brunel University, Uxbridge, Middlesex, UB8 3PH United Kingdom,*
[6]*Boston University, Boston, Massachusetts 02215,*
[7]*University of Cincinnati, Cincinnati, Ohio 45221,*
[8]*University of Colorado, Boulder, Colorado 80309,*
[9]*Columbia University, New York, New York 10533,*
[10]*Colorado State University, Ft. Collins, Colorado 80523,*
[11]*INFN Sezione di Ferrara and Universita di Ferrara, I-44100 Ferrara, Italy,*
[12]*INFN Lab. Nazionali di Frascati, I-00044 Frascati, Italy,*
[13]*University of Illinois, Urbana, Illinois 61801,*
[14]*Johns Hopkins University, Baltimore, MD 21218-2686,*
[15]*Lawrence Berkeley Laboratory, University of California, Berkeley, California 94720,*
[16]*Louisiana Technical University - Ruston,LA 71272,*
[17]*University of Massachusetts, Amherst, Massachusetts 01003,*
[18]*University of Mississippi, University, Mississippi 38677,*
[19]*Massachusetts Institute of Technology, Cambridge, Massachusetts 02139,*

[20] *Institute of Nuclear Physics, Moscow State University, 119899, Moscow Russia,*
[21] *Nagoya University, Chikusa-ku, Nagoya 464 Japan,*
[22] *University of Oregon, Eugene, Oregon 97403,*
[23] *Oxford University, Oxford, OX1 3RH, United Kingdom,*
[24] *INFN Sezione di Padova and Universita di Padova I-35100, Padova, Italy,*
[25] *INFN Sezione di Perugia and Universita di Perugia, I-06100 Perugia, Italy,*
[26] *INFN Sezione di Pisa and Universita di Pisa, I-56010 Pisa, Italy,*
[27] *Rutherford Appleton Laboratory, Chilton, Didcot, Oxon OX11 0QX United Kingdom,*
[28] *Rutgers University, Piscataway, New Jersey 08855,*
[29] *Stanford Linear Accelerator Center, Stanford University, Stanford, California 94309,*
[30] *Sogang University, Seoul, Korea,*
[31] *Soongsil University, Seoul, Korea 156-743,*
[32] *University of Tennessee, Knoxville, Tennessee 37996,*
[33] *Tohoku University, Sendai 980, Japan,*
[34] *University of California at Santa Barbara, Santa Barbara, California 93106,*
[35] *University of California at Santa Cruz, Santa Cruz, California 95064,*
[36] *University of Victoria, Victoria, B.C., Canada, V8W 3P6,*
[37] *Vanderbilt University, Nashville,Tennessee 37235,*
[38] *University of Washington, Seattle, Washington 98105,*
[39] *University of Wisconsin, Madison,Wisconsin 53706,*
[40] *Yale University, New Haven, Connecticut 06511.*